Lecture 14 Spring 1998

GEOCHRONOLOGY X: FISSON TRACK DATING

INTRODUCTION

Figure 14.1. Fission tracks in a polished and etched zircon. Photo courtesy J. M. Bird.

As we have already noted, a fraction of uranium atoms undergo spontaneous fission rather than alpha decay. The sum of the masses of the fragments is less than that of the parent U atom: this difference reflects the greater binding energy of the fragments. The missing mass has been converted to kinetic energy of the fission fragments. Typically, this energy totals about 200 MeV, a considerable amount of energy on the atomic scale. The energy is deposited in the crystal lattice through which the fission fragments pass by stripping electrons from atoms in the crystal lattice. The ionized atoms repel each other, disordering the lattice and producing a small channel and a wider stressed region in the crystal. The damage is visible as tracks seen with an electron microscope operating at magnifications of 50,000× or greater. However, the stressed region is more readily attacked and dissolved by acid; so by acid etching the tracks can be enlarged to the point where they are visible under the optical microscope. Figure 14.1 is an example. Because fission is a rare event in any case, fission track dating generally uses uranium rich minerals. Most work has been done on apatites, but sphene and zircon are also commonly used.

Fission tracks are subject to annealing at geologically low to moderate temperatures. In the absence of such annealing, the number of tracks is a simple function of time and the uranium content of the sample:

$$F_s = (\lambda_f/\lambda_\alpha)\,{}^{238}U\,(e^{\lambda_\alpha t} - 1) \qquad 14.1$$

where F_s is the number of tracks produced by spontaneous fission, ${}^{238}U$ is the number of atoms of ${}^{238}U$, λ_α is the α decay constant for ${}^{238}U$, and λ_f is the spontaneous fission decay constant, the best estimate for which is $8.46 \pm 0.06 \times 10^{-17}$ yr^{-1}. Thus about 5×10^{-7} U atoms undergo spontaneous fission for every one that undergoes α-decay. Equation 14.1 can be solved directly for t simply by determining the number of tracks and number of U atoms per volume of sample. In this case, t is the time elapsed since temperatures were high enough for all tracks to anneal. This is the basis of fission track dating. The temperatures required to anneal fission damage to a crystal are lower than those required to isotopically homogenize one. Thus fission track dating is typically used to "date" lower temperature events than conventional geochronometers.

ANALYTICAL PROCEDURES

Determining fission track density involves a relatively straightforward procedure of polishing and etching a thin section or grain mount, and then counting the number of tracks per unit area. A number of etching procedures have been developed for various substances. These are listed in Table 14.1. Track densities of up to several thousand per cm^2 have been recorded. A minimum density of 10 tracks per cm^2 is required for the results to be statistically meaningful. A fission track, which is typically 10 μ long, must intersect the surface to be counted. Thus equation 14.1 becomes:

$$\rho_s = F_s q = (\lambda_f/\lambda_\alpha)\,{}^{238}U\,(e^{\lambda_\alpha t} - 1)q \qquad 14.2$$

where ρ_s is the track density, q is the fraction of tracks intersecting the surface, and ${}^{238}U$ is now the concentration of ${}^{238}U$ per unit area.

The second step is determination of the U concentration of the sample. This is usually done by neutron irradiation and counting of the tracks resulting from neutron-induced fission. There are variations to this procedure. In one method, spontaneous fission tracks are counted, then the sample is heated to anneal the tracks, irradiated and recounted (this is necessary because irradiation heats the sample and results in partial annealing). Alternatively, a 'detector', either a U-free muscovite sample or a plastic sheet, is place over the surface of the polished surface that has previously been etched and counted. The sample together with the detector is irradiated, and the tracks in the detector counted. This avoids having to heat and anneal the sample. This latter method is more commonly employed.

TABLE 14.1. ETCHING PROCEDURES FOR FISSION TRACK DATING

Mineral	Etching Solution	Temperature (° C)	Duration
Apatite	5% HNO_3	25	10-30 s
Epidote	37.5M NaOH	159	150 min
Muscovite	48% HF	20	20 min
Sphene	Conc. HCl	90	30-90 min
Volcanic Glass	24% HF	25	1 min
Zircon	100M NaOH	270	1.25 h

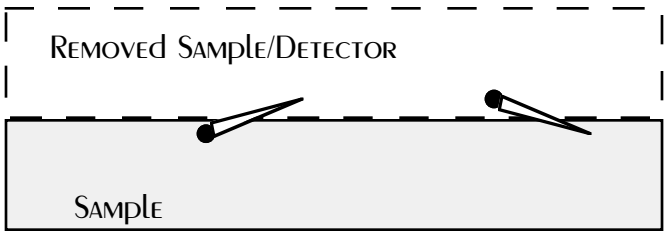

Figure 14.2. Geometry of the fission tracks in the detector method of U determination. Spontaneous fission tracks in the sample surface could have originated from either the existing sample volume, or the part of the sample removed by polishing. Tracks in the detector can only originate from the existing sample volume.

Whereas ^{238}U is the isotope that fissions in nature, it is actually ^{236}U, produced by neutron capture by ^{235}U, that undergoes neutron-induced fission. The number of ^{235}U fission events induced by thermal neutron irradiation is:

$$F_i = {}^{235}U\phi\sigma \qquad 14.3$$

where ϕ is the thermal neutron dose (neutron flux times time) and σ is the reaction cross section (about 580 barns for thermal neutrons). The induced track density is:

$$\rho_i = F_i q = {}^{235}U\phi\sigma q \qquad 14.4$$

Dividing equation 14.2 by 14.4 we have:

$$\frac{\rho_s}{\rho_i} = \frac{\lambda_f}{\lambda_\alpha}\frac{137.88}{\phi\sigma}(e^{\lambda_\alpha t} - 1) \qquad 14.5$$

In the detector method, equation 14.5 must be modified slightly to become:

$$\frac{\rho_s}{\rho_i} = \frac{\lambda_f}{\lambda_\alpha}\frac{137.88}{2\phi\sigma}(e^{\lambda_\alpha t} - 1) \qquad 14.6$$

The factor of two arises because surface-intersecting tracks produced by spontaneous fission originate both from U within the sample and from that part of the sample removed from etching. However, tracks in the detector can obviously only originate in the remaining sample. This is illustrated in Figure 14.2.

One of the most difficult problems in this procedure is correctly measuring the neutron dose. This is usually done by including a gold or aluminum foil and counting the decays of the radioisotope produced by neutron capture. Nevertheless, the neutron flux can be quite variable within a small space and it remains a significant source of error.

We can readily solve equation 14.6 for *t*:

$$t = \frac{1}{\lambda_\alpha} \ln\left[1 + \frac{\rho_s}{\rho_i}\frac{\lambda_\alpha}{\lambda_f}\frac{^{235}U}{^{238}U}2\phi\sigma\right] \qquad 14.7$$

and thus determine the time since the tracks last annealed.

Yet another alternative method is the *zeta method*, which involves comparison of spontaneous and induced fission track density against a standard of known age. The principle involved is no different from that used in many methods of analytical chemistry, where comparison to a standard eliminates some of the more poorly controlled variables. In the zeta method, the dose, cross section, and spontaneous fission decay constant, and U isotope ratio are combined into a single constant:

$$\zeta = \frac{\phi\sigma^{235}U}{\lambda_f{}^{238}U\rho_d} = \frac{\phi\sigma}{\lambda_f 137.88\rho_d} \qquad 14.8$$

where ρ_δ is the density of tracks measured in a glass standard. Standards used in the zeta method include zircon from the Fish Canyon Tuff (27.9 Ma), the Tardree rhyolite of Ireland (58.7 Ma), and South African kimberlites (82 Ma). The value of ζ is determined by analyzing standards of known age in every sample batch. ζ is determined from:

$$\zeta = \frac{e^{\lambda_\alpha t} - 1}{\lambda_\alpha(\rho_s/\rho_i)\rho_d} \qquad 14.9$$

The age is then calculated from:

$$t = \frac{1}{\lambda}\ln\left(1 + \frac{\zeta\lambda_\alpha\rho_s\rho_d}{\rho_i}\right) \qquad 14.10$$

Usually, fission track ages on a number of grains must be measured for the results to be significant. The results are often presented as histograms. Alternatively, when the errors are also considered, the results may be presented as a probability density diagram, such as Figure 14.3. Yet another approach is to plot the spontaneous track density (ρ_s) vs the induced track density (ρ_i), such as Figure 14.4. From equation 14.6, we see that the slope on such a diagram is proportional to time. Thus these kinds of plots are exactly analogous to conventional isochron diagrams. There is a difference, however. On a plot of ρ_s vs. ρ_i the intercept should be 0.

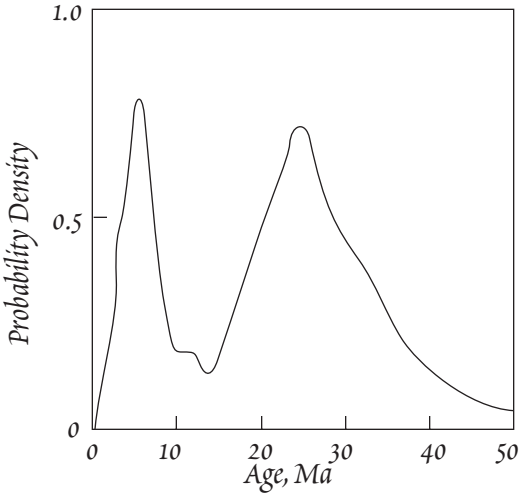

Figure 14.3. Probability density plot of fission track ages of 30 detrital zircon grains from the reworked El Ocote tephra from Mexico. The data show a bimodal distribution.

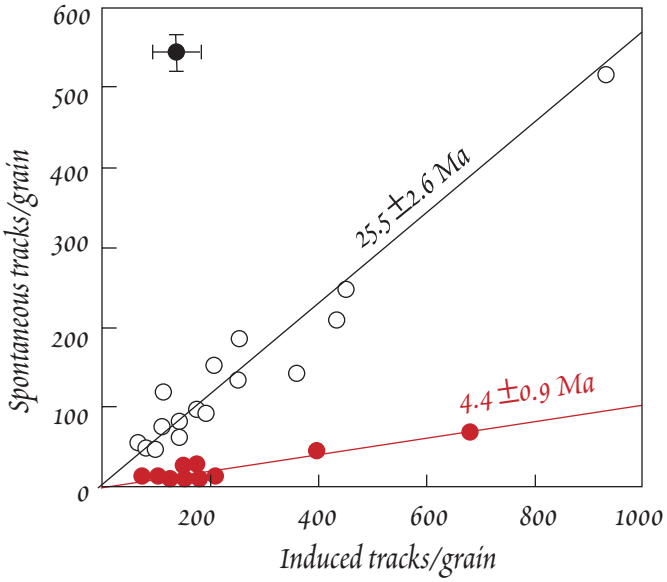

Figure 14.4. Spontaneous track density vs. induced track density for the same set of zircon grains as in Figure 14.3. On this plot, the slope of the correlation is proportional to time.

Interpreting Fission Track Ages

Fission tracks will anneal at elevated temperatures. As is the case for all chemical reaction rates, the annealing rate depends exponentially on temperature:

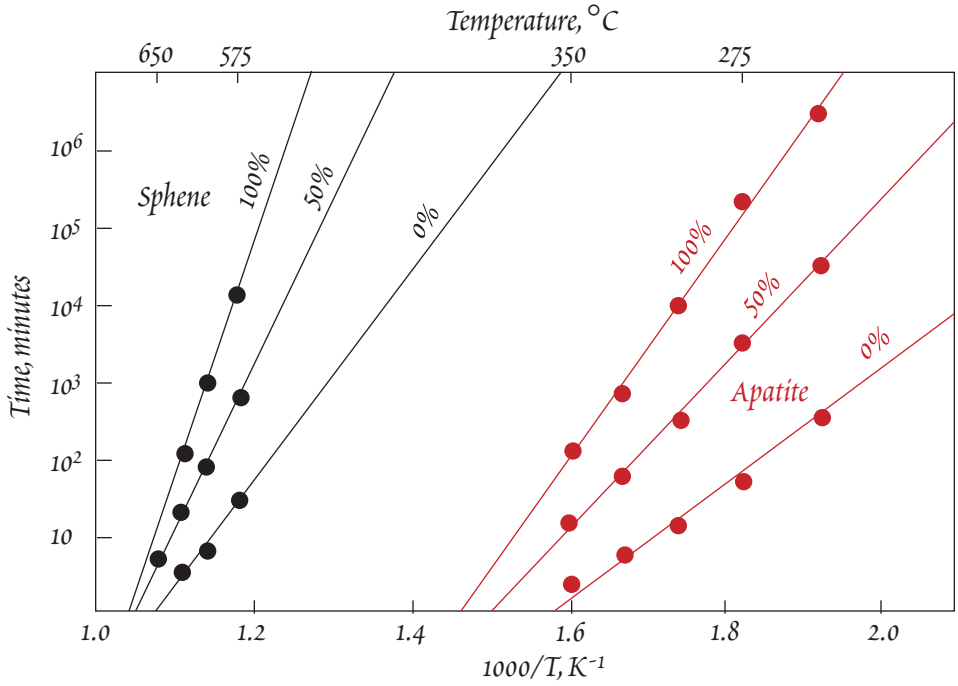

Figure 14.5. Relationship between the percentage of tracks annealed (lines labelled 100%, 50% and 0%), temperature, and time for apatite and sphere.

$$A = k \exp\left(\frac{E_A}{RT}\right) \qquad 14.11$$

where T is thermodynamic temperature (kelvins), k is a constant, R is the gas constant (some equations use k, Boltzmann's constant, which is proportional to R), and E_A is the activation energy. Thus, as is the case for conventional radiometric dating, fission track dating measures the time elapsed since some high temperature event. The constants k and E_A will vary from mineral to mineral, so that each mineral will close at different rates. In laboratory experiments, apatite begins to anneal around 70° C and anneals entirely on geologically short times at 175°C. Sphene, on the other hand, only begins to anneal at 275°C and does not entirely anneal until temperatures of 420°C are reached. In nature, a mineral held at high temperature will anneal very quickly: no fission tracks are retained. Figure 14.5 shows the experimental relationship between the percentage of tracks annealed, temperature, and time.

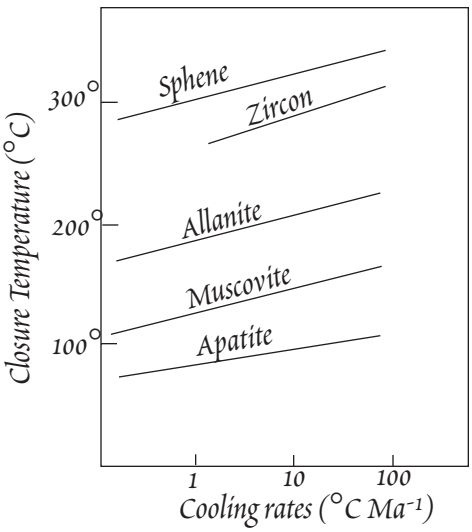

Figure 14.6. Apparent closure (annealing) temperatures of fission tracks as a function of cooling rate for a variety of minerals.

As temperature drops, tracks will be partially, but not entirely preserved. As we discussed in the context of K-Ar dating, the apparent closure temperature is a function of cooling rate. This cooling rate dependency is summarized in Figure 14.6. Because different methods of etching attack partially annealed tracks to different degrees, etching must be done in the same way a for closure temperature determination.

In general, closure temperatures for fission tracks are below those of conventional isotope geochronometers, so they are particularly useful in analysis of low temperature

events and in determining cooling histories. When combined with estimates of geothermal gradients, fission track ages, particularly if ages for a variety of minerals are determined, are a useful tool in studying uplift and erosion rates.

For example, the average fission track age for 3 apatites from the Huayna Potosi batholith in the Bolivian Andes is 12.5 Ma. We chose 10°C/Ma for a first order estimate of cooling rate and determine the closure temperature from Figure 14.4 to be 95°C. Assuming an average surface temperature of 10°C, we calculate the cooling rate to be:

$$\frac{dT}{dt} = \frac{95 - 10}{12.5} = 6.8°C/Ma \qquad 14.12$$

We could refine this value by re-estimating the closure temperature based on our result of 6.8°C/Ma. If we assume the geothermal gradient to be 30°C/km, we can calculate the exhumation rate to be:

$$\frac{dz}{dt} = \frac{dT/dt}{dT/dx} = \frac{6.8\ °C/Ma}{0.030\ °C/m} = 226\ m/Ma \qquad 14.13$$

Using this approach, exhumation rates have been estimated as 500 m/Ma over the past 10 Ma for the Alps and 800 m/Ma for the Himalayas. Figure 14.7 shows an example of the results of one such study of the Himalayas from northern India (Kashmir). Fission track ages of apatites from high grade metamorphic rocks of the Higher Himalaya Crystalline complex. A plot of ages vs. the altitude at which the samples were collected (Figure14.7) indicates an exhumation rate of 0.35 mm/a or 350 m/Ma over the last 7 million years.

As fission tracks anneal, they become shorter. Thus when a grain is subjected to elevated temperature, both the track density and the mean track length will decrease. As a result, problems of partial annealing of fission tracks can to some degree be overcome by also measuring the length of the tracks. Because (1) tracks tend to have a constant length (controlled by the energy liberated in the fission), (2) become progressively shorter during annealing, and (3) each track is actually a different age and has experienced a different fraction of the thermal history of the sample, the length distribution records information about the thermal history of the sample. Uniform track lengths suggest a simple thermal history of rapid cooling and subsequent low temperature (such as might be expected for a volcanic rock), while a broad distribution suggests a reheating event. A skewed distribution suggests initial slow cooling and subsequent low temperatures. Figure 14.8 illustrates how track lengths are expected to vary for a variety of hypothetical time-temperature paths.

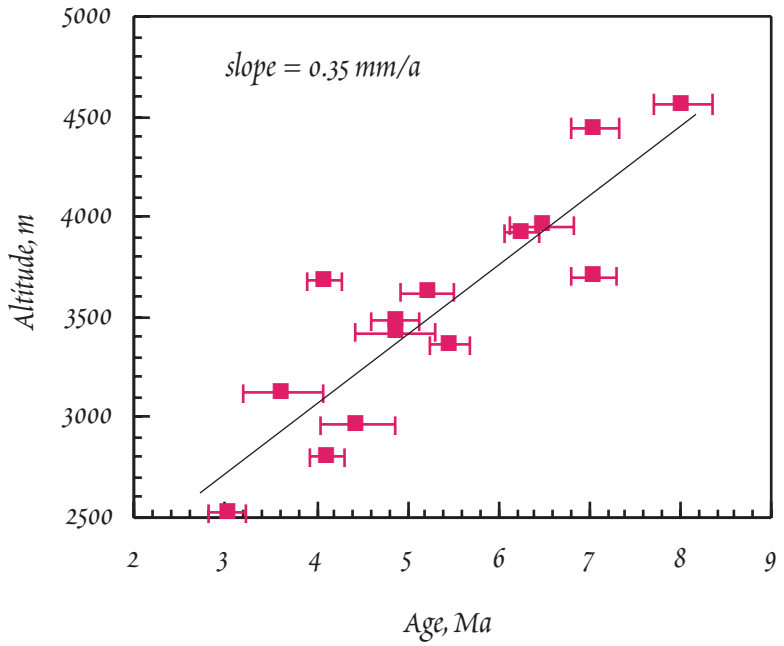

Figure 14.7. Apatite fission track ages vs. altitude for metamorphic rocks of the Higher Himalaya Crystalline belt of Kashmir. The correlation coefficient is 0.88. The slope indicates an uplift rate of 350 m/Ma. From Kumar et al. (1995).

One problem with the approach is that both etching rates and annealing rates, and therefore track lengths, depend on crystallographic orientation. As a result, track length measurements should be only on tracks having the same crystallographic orientation.

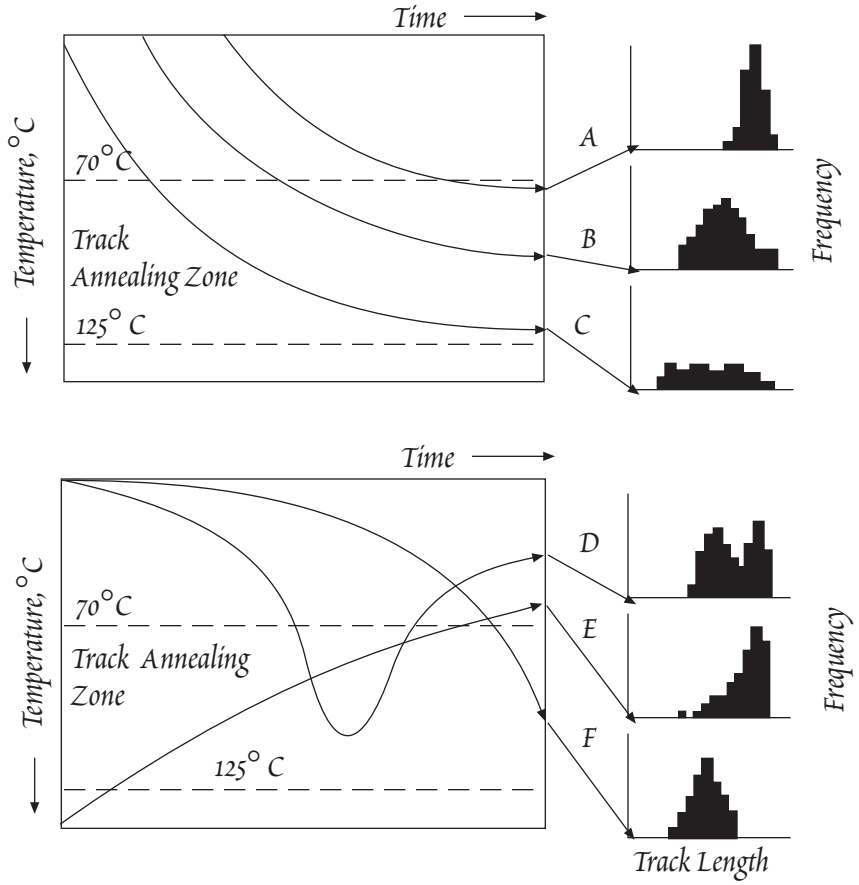

Figure 14.8. Hypothetical time-temperature paths and the distribution of track lengths that should result from these paths. From Ravenhurst and Donelick (1992).

REFERENCES AND SUGGESTIONS FOR FURTHER READING

Dickin, A. 1995. *Radiogenic Isotope Geochemistry*. Cambrige: Cambridge University Press.

Kumar, A., N. Lal, A. K. Jain and R. B. Sorkhabi. 1995. Late Cenozoic-Quarternary thermo-tectonic history of Higher Himalaya Crystalline (HHC) in Kishtwar-Padar-Zanskar region, NW Himalaya: evidence from fission track ages. *J. Geol. Soc. India*. 45: 375-391.

Ravenhurst, C. E. and R. A. Donelick.1992. Fission Track Thermochronology. in *Short Course Handbook on Low Temperature Thermochronology*, ed. M. Zentilli and P. H. Reynolds. 21-42. Nepean, Ontario: Mineral. Soc. Canada.

Zentilli, M. and P. H. Reynolds (ed.), 1992, *Short Course Handbook on Low Temperature Thermochronology*, Nepean, Ontario: Mineral. Soc. Canada.